

Cite this: *Nanoscale*, 2011, **3**, 2718

www.rsc.org/nanoscale

PAPER

Polarisation stabilisation of vertical cavity surface emitting lasers by minimally invasive focused electron beam triggered chemistry

Ivo Utke,^{*a} Martin G. Jenke,^a Christian Röling,^b Peter H. Thiesen,^b Vladimir Iakovlev,^c Alexei Sirbu,^c Alexandru Mereuta,^c Andrei Caliman^c and Eli Kapon^c

Received 14th January 2011, Accepted 10th February 2011

DOI: 10.1039/c1nr10047e

Local electron triggered reactions of functional surface adsorbates were used as a maskless, dry, and minimally invasive nanolithography concept to stabilize the polarisation of individual vertical cavity surface emitting lasers (VCSELs) on a wafer in a post-processing step. Using a 30 keV focused electron beam of a scanning electron microscope and injecting volatile organo-metallic $(\text{CH}_3)_2\text{Au}(\text{tfa})$ molecules, polarisation gratings were directly written on VCSELs by dissociating the surface adsorbed molecules. The electron triggered adsorbate dissociation resulted in electrically conductive Au-C nanocomposite material, with gold nanocrystals embedded in a carbonaceous matrix. A resistivity of $2500 \mu\Omega\text{cm}$ was measured at a typical composition of 30 at.% Au. This material proved successful in suppressing polarisation switching when deposited as line gratings with a width of 200 nm, a thickness of 50 nm, and a pitch of 500 nm and $1 \mu\text{m}$. Refractive index measurements suggest that the optical attenuation by the deposited Au-C material is much lower than by pure Au thus giving a low emission power penalty while keeping the polarisation stable.

Introduction

The possibility to deposit or remove very small amounts of material for trimming purposes on a fully processed micro/nanodevice at the right place at will without interference to surrounding sensitive areas can be very cost effective even if the speed of the deposition (or etching) is very low compared to standard photolithography. In this article, we describe an emerging lithography concept, based on gas-assisted focused electron beam induced deposition (FEBID),¹ which enables local deposition of conductive material for refining the performance of a micro-optical device, a vertical-cavity surface-emitting laser (VCSEL), see Fig. 1. Long-wavelength emitting VCSELs in the 1310 nm range offer numerous advantages for applications in local and access networks and optical spectroscopy thanks to their low power consumption, high speed modulation, and ease of coupling to optical fibers.² However, due to the cylindrical symmetry of these devices typically made on standard (100) GaAs or InP substrates, they suffer from the lack of a stable polarisation state and hence the polarisation can flip along orthogonal (100) directions during operation, *i.e.* during current

injection. Approaches for achieving polarisation control in VCSELs comprised non-isotropic gain using (311) substrates³ and non-cylindrical resonators.⁴ Classical, resist-based e-beam lithography approaches were also used to fabricate polarisation stabilizing line gratings on the VCSEL's distributed Bragg reflectors (DBRs) in combination with metal lift-off⁵ or deep reactive ion etching.⁶ However, using above methods, 100%

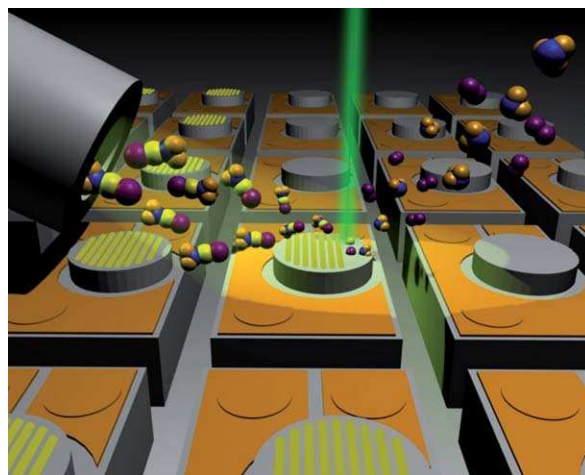


Fig. 1 Gas-assisted focused electron beam induced deposition for laser refining. By scanning the focused electron beam, polarisation gratings can be deposited on top of individual VCSELs without the need for masks, lithography resist removal, or wet chemistry steps.

^aEMPA, Swiss Federal Laboratories for Materials Science and Technology, Feuerwerkerstrasse 39, CH-3602 Thun, Switzerland. E-mail: Ivo.Utke@empa.ch; Fax: +41 21332284490; Tel: +41 332282957

^bAccurion GmbH, Göttingen, Germany. E-mail: pt@accurion.com; Fax: +49(0)5519996010; Tel: +49(0)551999600

^cEPFL SB ICMP LPN, PH D3 424 (Bâtiment PH), Station 3, CH-1015 Lausanne, Switzerland. E-mail: eli.kapon@epfl.ch; Fax: +41 216934525; Tel: +41 216933321

yields were not achieved; moreover, a post-process method which could trim individual VCSEL devices to achieve standard emission output is preferable.

We will demonstrate here that the FEBID lithography process illustrated in Fig. 1 is a viable method for depositing line gratings on top of individual VCSELs such that their polarisation state can be adjusted. The technique relies on the local dissociation of functional, volatile, surface physisorbed molecules by a focused electron beam. The volatile dissociation reaction products desorb into the vacuum chamber of the scanning electron microscope (SEM) and are removed by the vacuum system, while the non-volatile dissociation products form the deposit. Since the molecules are continuously supplied to the substrate surface *via* a gas injection system, the deposition can be continued to produce to (almost) any desired three-dimensional deposit shape by moving the focused electron beam or keeping it stationary. Once the desired structure is written, the gas injection system is closed and the non-dissociated molecules desorb, leaving the desired lithographic deposit pattern on the surface.

This nanolithography concept is, by its nature, maskless and single step in contrast to standard resist based lithography and lift-off procedures. It does not require any wet chemical step, does not implant any material (which is the case when using focused Ga-ion beams) and thus is minimally invasive to sensitive underlying and surrounding structures and devices.

While dissociation of molecules by electrons is a long studied subject extending several fundamental science fields, including DNA radiolysis and related genotoxic damage,⁷ surface science,^{8,9} auto-catalysis,¹⁰ self-assembled monolayers,¹¹ and semiconductor process plasmas,¹² its potential for an electron-controlled chemical lithography concept was intensely studied only recently, both for nanoscale deposition and etching, see reviews.^{13–17} Recent device prototypes demonstrate the flexibility in shape and material deposited by FEBID: magnetic sensors for bead detection,¹⁸ nanopores for DNA sequencing,¹⁹ plasmonic antennae,^{20,21} plasmonic-photonic nanodevices for label-free detection of molecules,²² graphenoid membranes,²³ single-crystal nanowires,²⁴ and tunable strain sensors.²⁵ In semiconductor industry FEBID processes are used for in-line 45 nm node photomask repair.²⁶ Recent impressive progress in FEBID technology comprises the control over shape down to the nanometre scale using *in situ* detection schemes,²⁷ automation protocols for wafer processing,²⁸ and the control over material purity and nanocomposite composition *via* co-injection of reactive and organic gases.^{29–32}

Experimental

The VCSELs in this study emitted at 1310 nm wavelength. They had an InAlGaAs/InP multi-quantum well active region and a p++/n++ InAlGaAs regrown tunnel junction for optical and electrical confinements. The non-doped AlGaAs DBRs were fused to the InP-based cavity using a localized double wafer fusion process.^{33,34} These VCSELs have been demonstrated to be suitable for high speed telecommunication applications, with good performance obtained at 10 Gb s⁻¹ modulation speeds up to 100 °C.³⁵

FEBID of polarisation stabilizing gratings on top of the VCSELs was carried out in a dual beam FIB/SEM (Lyra Tescan)

with a tungsten filament operating at 30 kV for best lateral resolution. With a gas injection system (Aleminis) equipped with an internal reservoir, the vapour molecules of dimethyl-Au-trifluoroacetylacetonate, (CH₃)₂-Au(O₂C₅H₄F₃), (CAS 63470-53-1), were directed to the VCSEL. The impinging molecule flux was around 1 × 10¹⁷ molecule cm⁻² s with the nozzle positioned 100 μm close to the VCSEL. Exposure time and position of the electron beam were controlled using lithography software. A beam current of 100 pA was used for grating wire deposition in multiple scans (800 ns dwell time, 10 ms refresh time). The material composition was determined by energy dispersive X-ray spectrometry (EDX) and the wire geometry was determined by focused ion beam (FIB) cross-sectioning. Refractive index measurements of the nanocomposite FEBID material were performed with a spectroscopic imaging ellipsometer (nanofil_ep3se, Accurion GmbH, Göttingen).

Results and Discussion

VCSEL Polarisation

Fig. 2 shows two typical examples of a successful suppression of polarisation switching by a FEB deposited polarisation gratings. The polarisations 0° and 90° refer to the principle

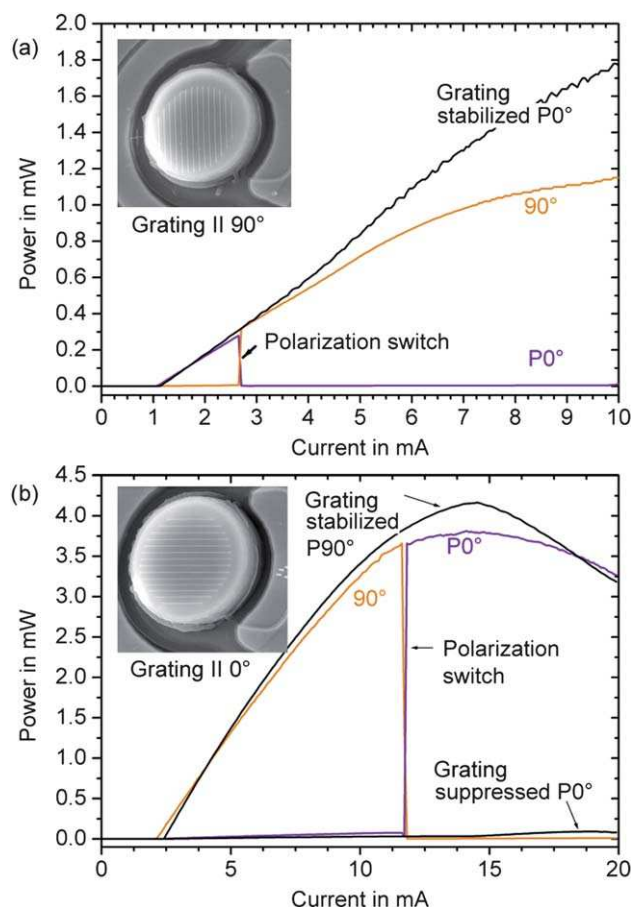


Fig. 2 Suppression of polarisation switching in VCSELs by grating deposition parallel to the unwanted polarisation direction. The pitch distance is 1 μm. The insets show SEM tilt views of the FEB deposited gratings on the VCSELs' top DBR mirrors. (a) Grating stabilizes 0° polarisation. (b) Grating stabilizes 90° polarisation.

crystallographic axes [100] and [010] of the (100) oriented wafer, respectively, from which the VCSELs were fabricated. The gratings must be aligned parallel to the electric field vector of an unwanted polarisation mode in order to suppress it; the polarisation selection mechanism is then brought about mainly by increased cavity losses for this optical mode. The increase in power and threshold current of the stabilized mode seen in Fig. 2a and b could be attributed to a decrease in the reflectivity of the output mirror due to the formation of the grating. The exact reason for this behaviour is currently subject of ongoing simulation work.

The total length of all grating wires together was 180 μm per VCSEL. The grating wire pitch was 1 μm , and the wire was 200 nm wide at full width at half maximum (FWHM) and 80 nm thick. This yields a total deposited volume of roughly 3 μm^3 . Since optimized deposition yields for FEBID range around 0.025 μm^3 per nanocoulomb,³⁶ this volume could be written within about two minutes using a field emission electron source microscope at 1 nA electron beam current. As we used a tungsten-source equipped microscope at 100 pA current, the total deposition time was about a factor 10 higher in our experiments. With respect to fabrication throughput it is worth to mention that the single electron beam approach, presented here for feasibility, could be upscaled to wafer scale level. Presently, massively parallel multi-electron-beam systems have been developed as a next generation, maskless lithography concept operating with 200 to 10 000 electron beams^{37–39} for classical resist exposure. If adapted to resistless gas-assisted FEBID, simultaneous fabrication of gratings on many VCSELs could be performed.

A thin halo deposit along the wires can be observed which is due to backscattered primary electrons exiting the surface. The backscattered electron yield from a 30 keV primary electron beam impinging on GaAs is 32.8% and their lateral exit radius measured from the centre of the impinging focused electron beam is about 3.6 μm . Since the halo will simply absorb the VCSEL emitted light and will not contribute to polarisation stabilisation, it would be desirable to prevent its deposition. This can be achieved by low-energy electron beams; for instance, for a 1 keV impinging primary electron beam the lateral BSE exit range is only 12 nm in GaAs. However, with tungsten filament equipped SEMs the beam size becomes unacceptably large at such energies⁴⁰ which prevented us from depositing in these more favourable conditions. Fig. 3 shows that polarisation can also be forced *against* the naturally stable polarisation axis of the VCSEL. FEBID gives thus the freedom to choose the individual laser polarisation using a post-process step, decoupled from the industrial VCSEL wafer fabrication. The wire grating pitch was 550 nm, the thickness 100 nm and the width at FWHM 165 nm.

Generally, it was found that FEB deposited grating wires with 550 nm pitch distance and a width of around 160 nm had to have a minimum thickness of around 30 nm to make a visible effect in the power vs. current diagrams of VCSELs. At this minimum thickness polarisation switching was not yet fully suppressed but shifted to lower or higher injection currents depending on the mutual orientation of the grating wires and the initially stable polarisation axis at low injection current. Further studies will seek to push to the resolution limits of sub-10 nm reported for FEBID of grating wire widths on membranes.²⁷ If such small

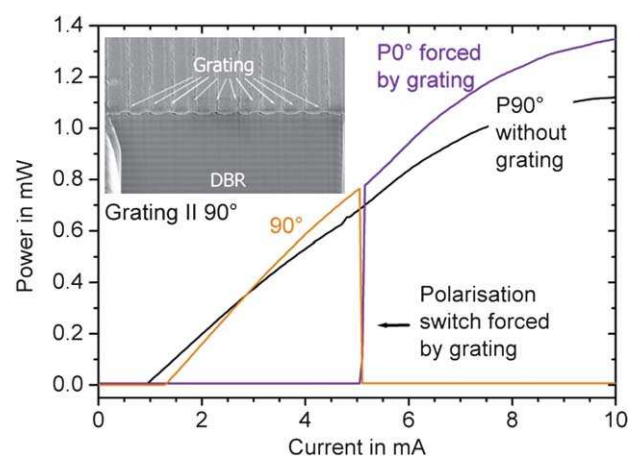


Fig. 3 Forced 0°-polarisation for injection currents >5.4 mA. Without grating the VCSEL showed stable 90° polarisation for all injection currents. Inset: SEM tilt view of FIB cross-section of VCSEL (with top DBR) with FEB deposited polarisation grating having a 550 nm pitch.

wires would prove to stabilize polarisation, further gains in fabrication throughput could be expected due to the fact that less material needs to be deposited.

Analysis of FEBID material

The material deposited by a 30 keV electron beam using the $(\text{CH}_3)_2\text{-Au}(\text{O}_2\text{C}_5\text{H}_4\text{F}_3)$ molecule was measured to be composed of about 30 at.% Au, 60 at.% C, and 10 at.% O. The inset in Fig. 4 shows a dark field transmission electron microscopy image of the nanocomposite structure typically obtained from this organometallic molecule under electron dissociation. It was observed that gold nanocrystals were embedded in an amorphous carbonaceous matrix. The gold nanocrystal size was distributed around 2 nm which could be concluded from the thinnest edge parts where separate grains could be resolved. The Au/C-nanocomposite structure was obtained since not only metal–ligand bonds were dissociated by electrons but also co-dissociation of intra-ligand bonds occurred which led to non-volatile fragments forming the amorphous carbonaceous matrix. The electrical resistivity of the grating wires was measured to be 2500 $\mu\Omega\text{ cm}$ in two-point measurements, being about 1000 times larger than pure bulk gold.

In principle, there are routes to increase the FEB triggered reaction outcome of metal content by using additional reactive gases like oxygen, water, or atomic hydrogen^{30,31,41} and by injecting carbon-free inorganic molecules, like AuClPF_3 ⁴² or $\text{Pt}(\text{PF}_3)_4$.⁴³

However, as was experimentally shown above, the present nanocomposite material was already well suited for VCSEL polarisation stabilization. Measurements of the complex refractive index, $\tilde{n} = n + ik$, are shown in Fig. 4 together with the values for bulk gold⁴⁴ for comparison. At the telecom's long-wavelength range above 900 nm the optical properties of our FEB deposited Au/C nanocomposite seem to be favourable with respect to pure gold since a low light attenuation by absorption can be expected due to the low k -value, hence the emission power penalty should be smaller. In general, the wavelength dependencies of n and k of

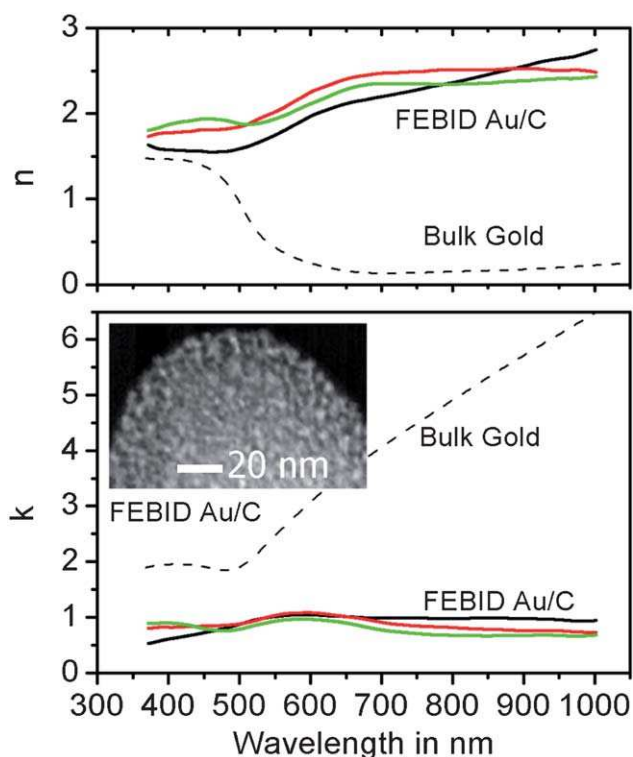


Fig. 4 Real and imaginary parts of the complex refractive index of Au/C nanocomposites as obtained from micro-ellipsometry measurements. For comparison bulk gold values (dashed line) are given. The inset shows the nanocomposites nature of the FEBID material: Au-nanocrystals (light spots) are embedded in an amorphous carbonaceous matrix. The image was taken in the dark field mode of a transmission electron microscope.

the FEBID Au/C nanocomposite material shows similarities with thin colloidal gold layers,⁴⁵ especially the low, yet peaked k value and the high n value with respect to bulk gold. However, while the thin colloidal gold films showed a peak for n around 600 nm, probably due to plasmon resonances, such a peak was not observed in our nanocomposites. On absolute scale, FEBID deposits showed larger n and k values compared to colloidal gold films, probably due to the additional carbonaceous matrix present in our material.

Conclusions

We have demonstrated the potential of FEBID as lithographical concept for minimally invasive, nanoscale post-processing of long-wavelength, high-speed telecom VCSELs, specifically for refining the polarisation of the output beam without noticeable power penalty. The nanocomposite FEBID material is functional and further experiments and simulations will seek to optimise the metal-to-carbon ratio and the metal nanocrystal size with respect to polarisation stabilisation and minimum amount of material to be deposited. No detrimental effect of electron irradiation on laser emission properties was observed.

Acknowledgements

We would like to acknowledge the synthesis of the organo-metallic gold molecule by S. Krauss and thank G. Bürki for FIB

cross-sections. This work was supported in part by the European Project MOSEL and the CTI project (No. 10710.1 PFNM-NM).

References

- I. Utke and A. Gözhäuser, *Angew. Chem., Int. Ed.*, 2010, **49**, 9328–9330.
- E. Kapon and A. Sirbu, *Nat. Photonics*, 2009, **3**, 27–29.
- C. Caneau, N. Nishiyama, G. Guryanov, C. E. Zah, B. Hall and R. Bhat, *Conference Proceedings—International Conference on Indium Phosphide and Related Materials*, Glasgow, Scotland, 2005, pp. 660–663.
- M.-C. Amann and M. Ortsiefer, *Phys. Status Solidi A*, 2006, **203**, 3538–3544.
- C. A. Berseth, B. Dwir, I. Utke, H. Pier, A. Rudra, V. P. Iakovlev, E. Kapon and M. Moser, *J. Vac. Sci. Technol., B*, 1999, **17**, 3222–3225.
- V. Iakovlev, A. Syrbu, A. Mereuta, A. Caliman, K. Atlasov, A. Mircea, B. Dwir and E. Kapon, *Conference on Lasers and Electro-Optics & Quantum Electronics and Laser Science Conference*, vol. 1–9, 2008, pp. 2287–2288.
- B. Boudaiffa, P. Cloutier, D. Hunting, M. A. Huels and L. Sanche, *Science*, 2000, **287**, 1658–1660.
- J. D. Wnuk, S. G. Rosenberg, J. M. Gorham, W. F. van Dorp, C. W. Hagen and D. H. Fairbrother, *Surf. Sci.*, 2011, **605**, 257–266.
- T. Hamann, E. Böhler and P. Swiderek, *Angew. Chem., Int. Ed.*, 2009, **48**, 4643–4645.
- M. M. Walz, M. Schirmer, F. Vollnhals, T. Lukasczyk, H. P. Steinrück and H. Marbach, *Angew. Chem., Int. Ed.*, 2010, **49**, 4669–4673.
- A. Turchanin, D. Käfer, M. El-Desawy, C. Wöll, G. Witte and A. Gözhäuser, *Langmuir*, 2009, **25**, 7342–7352.
- L. G. Christophorou and J. K. Olthoff, *Fundamental Electron Interactions with Plasma Processing Gases*, Kluwer Academic/Plenum Publishers, New York, 1st edn, 2004.
- N. J. Mason, *Int. J. Mass Spectrom.*, 2008, **277**, 31–34.
- I. Utke, P. Hoffmann and J. Melngailis, *J. Vac. Sci. Technol., B*, 2008, **26**, 1197–1276.
- A. Botman, H. Mulders and C. W. Hagen, *Nanotechnology*, 2009, **20**, 372001.
- W. F. van Dorp and C. W. Hagen, *J. Appl. Phys.*, 2008, **104**, 081301.
- S. J. Randolph, J. D. Fowlkes and P. D. Rack, *Crit. Rev. Solid State Mat. Sci.*, 2006, **31**, 55–89.
- M. Gabureac, L. Bernau, I. Utke and G. Boero, *Nanotechnology*, 2010, **21**, 115503.
- C. Danelon, C. Santschi, J. Brugger and H. Vogel, *Langmuir*, 2006, **22**, 10711–10715.
- A. Weber-Bargioni, A. Schwartzberg, M. Schmidt, B. Harteneck, D. F. Ogletree, P. J. Schuck and S. Cabrini, *Nanotechnology*, 2010, **21**, 065306.
- S. Graells, S. Acimovic, G. Volpe and R. Quidant, *Plasmonics*, 2010, **5**, 135–139.
- F. De Angelis, G. Das, P. Candeloro, M. Patrini, M. Galli, A. Bek, M. Lazzarino, I. Maksymov, C. Liberale, L. C. Andreani and E. Di Fabrizio, *Nat. Nanotechnol.*, 2010, **5**, 67–72.
- A. Turchanin, A. Beyer, C. T. Nottbohm, X. Zhang, R. Stosch, A. Sologubenko, J. Mayer, P. Hinze, T. Weimann and A. Gözhäuser, *Adv. Mater.*, 2009, **21**, 1233–1237.
- K. L. Klein, S. J. Randolph, J. D. Fowlkes, L. F. Allard, H. M. Meyer III, M. L. Simpson and P. D. Rack, *Nanotechnology*, 2008, **19**, 345705.
- C. H. Schwalb, C. Grimm, M. Baranowski, R. Sachser, F. Porrati, H. Reith, P. Das, J. Müller, F. Volklein, A. Kaya and M. Huth, *Sensors*, 2011, **10**, 9847–9856.
- C. Ehrlich, U. Buttgerit, K. Boehm, T. Scheruebl, K. Edinger and T. Bret, *Proc. SPIE*, 2008, **6792**, H7920.
- W. F. Van Dorp, S. Lazar, C. W. Hagen and P. Kruit, *J. Vac. Sci. Technol., B*, 2007, **25**, 1603–1608.
- J. H. Kindt, G. E. Fantner, J. B. Thompson and P. K. Hansma, *Nanotechnology*, 2004, **15**, 1131–1134.
- A. Perentes and P. Hoffmann, *Chem. Vap. Deposition*, 2007, **13**, 176–184.
- A. Botman, M. Hesselberth and J. J. L. Mulders, *Microelectron. Eng.*, 2008, **85**, 1139–1142.

-
- 31 H. Miyazoe, I. Utke, H. Kikuchi, S. Kiri, V. Friedli, J. Michler and K. Terashima, *J. Vac. Sci. Technol., B*, 2010, **28**, 744–750.
- 32 L. Bernau, M. Gabureac, R. Erni and I. Utke, *Angew. Chem., Int. Ed.*, 2010, **49**, 8880–8884.
- 33 V. Iakovlev, G. Suruceanu, A. Caliman, A. Mereuta, A. Mircea, C. A. Berseth, A. Syrbu, A. Rudra and E. Kapon, *IEEE Photonics Technol. Lett.*, 2005, **17**, 947–949.
- 34 A. Sirbu, V. Iakovlev, A. Mereuta, A. Caliman, G. Suruceanu and E. Kapon, *Semicond. Sci. Technol.*, 2011, **26**, 014016.
- 35 A. Mereuta, G. Suruceanu, A. Caliman, V. Iacovlev, A. Sirbu and E. Kapon, *Opt. Express*, 2009, **17**, 12981–12986.
- 36 S. Lipp, L. Frey, C. Lehrer, B. Frank, E. Demm, S. Pauthner and H. Ryssel, *J. Vac. Sci. Technol., B*, 1996, **14**, 3920–3923.
- 37 A. Mohammadi-Gheidari, C. W. Hagen and P. Kruit, *J. Vac. Sci. Technol., B*, 2010, **28**, C6G5–C6G10.
- 38 E. Platzgummer, S. Cernusca, C. Klein, J. Klikovits, S. Kvasnica and H. Loeschner, *Proc. SPIE*, 2010, **7823**, 782308.
- 39 M. J. Wieland, G. De Boer, G. F. Ten Berge, M. Van Kervinck, R. Jager, J. J. M. Peijster, E. Slot, S. W. H. K. Steenbrink, T. F. Teepe and B. J. Kampherbeek, *Proc. SPIE*, 2010, **7637**, 76370F.
- 40 P. Hoffmann, I. Utke, F. Cicoira, B. Dwir, K. Leifer, E. Kapon and P. Doppelt, *Mater. Res. Soc. Symp.–Proc.*, 2000, **624**, 171–177.
- 41 K. Molhave, D. N. Madsen, A. M. Rasmussen, A. Carlsson, C. C. Appel, M. Brorson, C. J. H. Jacobsen and P. Boggild, *Nano Lett.*, 2003, **3**, 1499–1503.
- 42 I. Utke, P. Hoffmann, B. Dwir, K. Leifer, E. Kapon and P. Doppelt, *J. Vac. Sci. Technol., B*, 2000, **18**, 3168–3171.
- 43 J. D. Barry, M. Ervin, J. Molstad, A. Wickenden, T. Brintlinger, P. Hoffman and J. Meingailis, *J. Vac. Sci. Technol., B*, 2006, **24**, 3165–3168.
- 44 P. B. Johnson and R. W. Christy, *Phys. Rev. B: Solid State*, 1972, **6**, 4370–4379.
- 45 E. S. Kooij, H. Wormeester, E. A. M. Brouwer, E. van Vroonhoven, A. van Silfhout and B. Poelsema, *Langmuir*, 2002, **18**, 4401–4413.